Neuron, Volume *78*

Supplemental Information

Arc/Arg3.1 Is a Postsynaptic Mediator of Activity-Dependent Synapse Elimination in the Developing Cerebellum

Takayasu Mikuni, Naofumi Uesaka, Hiroyuki Okuno, Hirokazu Hirai, Karl Deisseroth, Haruhiko Bito, and Masanobu Kano

Supplemental Inventory

SUPPLEMENTAL FIGURES

Figure S1, related to Figure 1.

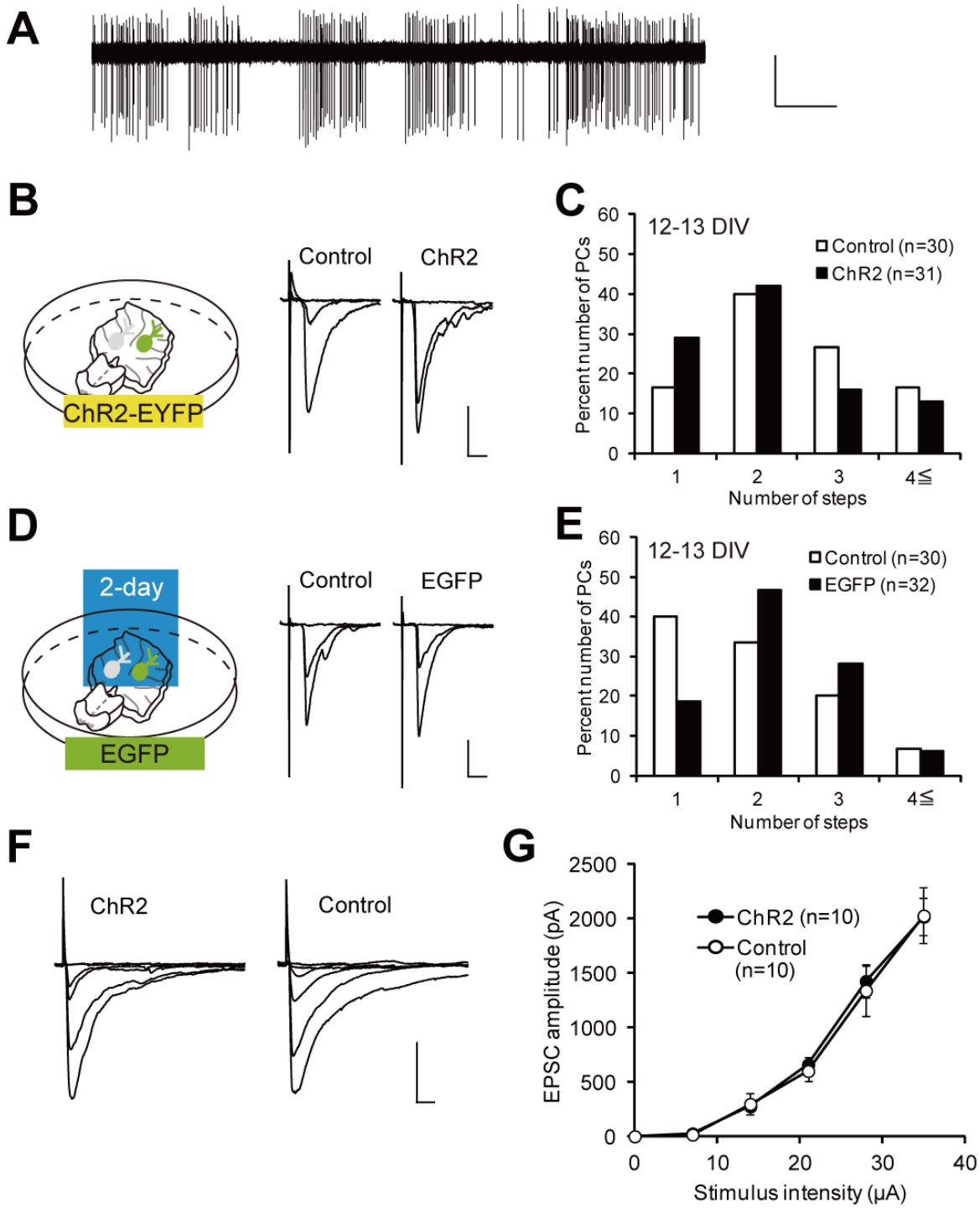

Figure S1, related to Figure 1.

Control Experiments for the Acceleration of CF Synapse Elimination Caused by Elevation of PC Activity (A-E) and Normal PF-PC Synaptic Transmission in Photostimulated PCs (F and G)

(A) Representative cell-attached extracellular recording from a PC in a olivo-cerebellar coculture at 10 DIV. Scale bars, 0.5 s and 50 pA.

(B) ChR2 was expressed in PCs but no light was applied during culturing. CF-EPSCs recorded in a control (left, with 2 distinct EPSC steps) and a ChR2-expressing (right, with 2 distinct EPSC steps) PC. Scale bars, 10 ms and 1 nA. Holding potential, -30 mV.

(C) Frequency distribution histogram for the number of CFs innervating control (open columns, n = 30) and ChR2-expressing (filled columns, n = 31) PCs from 20 cocultures. There was no significant difference in frequency distribution between the two groups of PCs (P = 0.2232, Mann-Whitney U test).

(D) EGFP was expressed in PCs and blue light (1 s light exposure at 0.1 Hz) was applied for two days from 10 or 11 DIV. CF-EPSCs recorded in a control (left, with 2 distinct EPSC steps) and an EGFP-expressing (right, with 2 distinct EPSC steps) PC. Scale bars, 10 ms and 1 nA. Holding potential, -30 mV.

(E) Frequency distribution histogram for the number of CFs innervating control (open columns, n = 30) and EGFP-expressing (filled columns, n = 32) PCs from 19 cocultures. There was no significant difference in frequency distribution between the two groups of PCs (P = 0.1596, Mann-Whitney U test).

(F and G) Input-output relationship of PF-EPSCs. There was no significant difference between photostimulated (black, n = 10) and control (white, n = 10) PCs from 7 cocultures (P = 0.7800, two-way ANOVA). Scale bars, 10 ms and 1 nA. Holding potential, -70 mV. Data are expressed as mean ± SEM.

Figure S2, related to Figure 2.

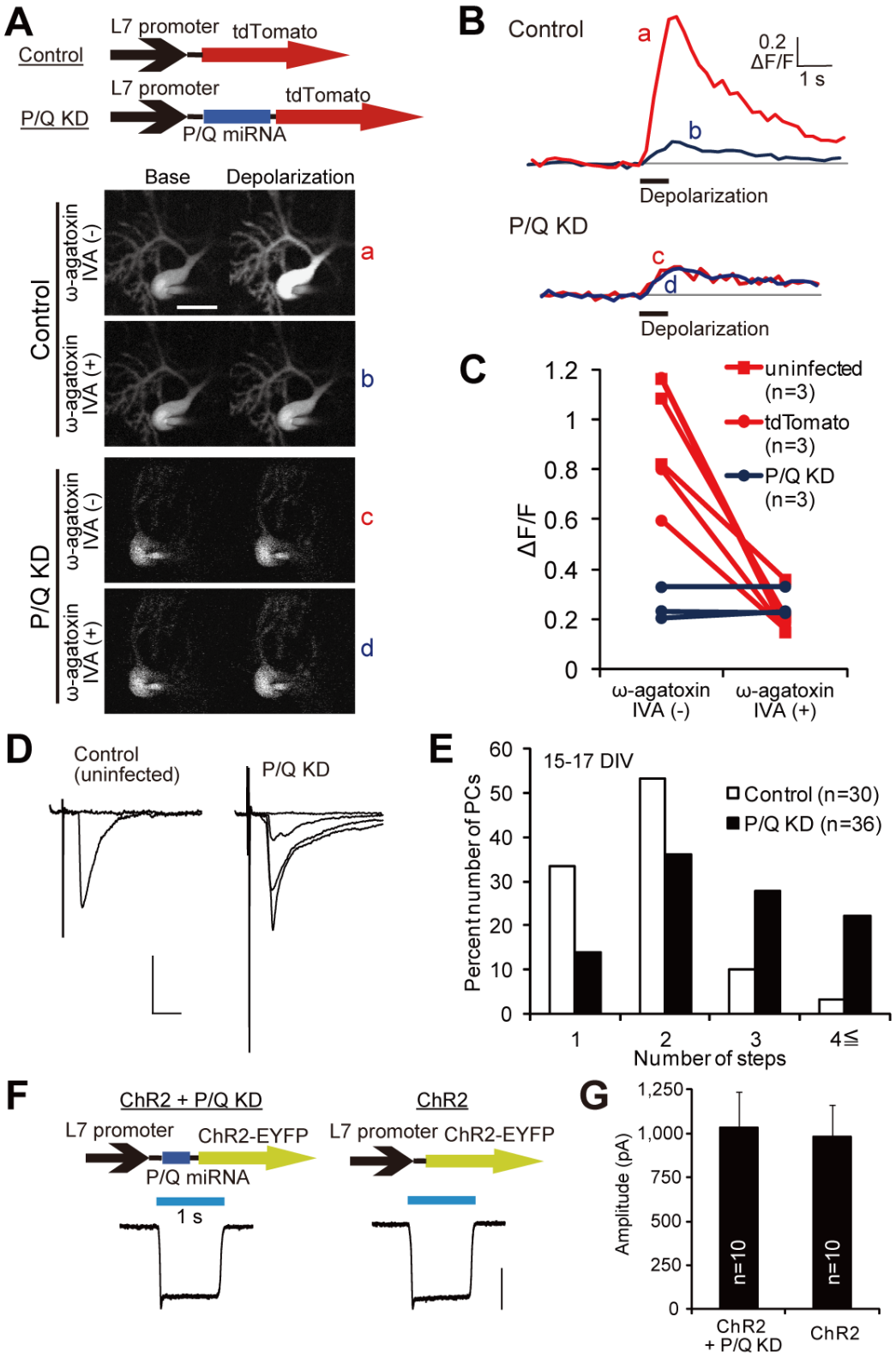

Figure S2, related to Figure 2.

P/Q-Type VDCCs Mediate CF Synapse Elimination in Cocultures

(A) P/Q miRNA and a fluorescent protein, tdTomato are driven by L7 promoter for PC-specific P/Q knockdown ("P/Q KD"). PCs were loaded with a Ca^{2+} indicator dye (Oregon Green BAPTA-1, 0.2 mM) through patch pipettes. Ca^{2+} signals were measured from the soma before and after direct depolarization from -70 mV to 0 mV for 1 s, before and after the application of ω-agatoxin IVA (0.4 μM). Scale bar, 20 μm.

(B) Representative Ca^{2+}-dependent fluorescent signals from a control PC (tdTomato, upper) and a PC with P/Q KD (P/Q miRNA and tdTomato, lower). Ca^{2+} influx after depolarization was smaller in the P/Q KD PC. Bath-applied ω-agatoxin IVA robustly decreased Ca^{2+} transients in the control PC, while ω-agatoxin IVA caused little change in the P/Q KD PC.

(C) Summary graph for peak Ca^{2+} transients before and after application of ω-agatoxin IVA (uninfected: 3 cells, tdTomato-expressing: 3 cells, and P/Q KD: 3 cells). Ca^{2+} transients through P/Q-type VDCCs were abolished in P/Q KD PCs ($P < 0.0001$, Student's t test, comparison of ΔF/F(ω-agatoxin +) /ΔF/F(ω-agatoxin -) between control (uninfected and tdTomato-expressing) and P/Q KD PCs).

(D) Specimen records of CF-EPSCs recorded in a control (left, with 1 EPSC step) and a P/Q KD (right, with 3 distinct EPSC steps) PC. Scale bars, 10 ms and 1 nA. Holding potential, -30 mV.

(E) Frequency distribution histogram for the number of CFs innervating control (open columns, n = 30) and P/Q KD (filled columns, n = 36) PCs from 28 cocultures. Frequency distribution was significantly different between the two groups of PCs ($P = 0.0017$, Mann-Whitney U test).

(F) Voltage-clamp recording of inward current from a ChR2-expressing PC (right, "ChR2") and a ChR2 plus P/Q miRNA-coexpressing PC (left, "ChR2 + P/Q KD") in response to 1-s blue light stimulation. Holding potential, -70 mV. Scale bar, 500 pA.

(G) Summary graph for the amplitude of light-evoked inward currents in the two groups of PCs (ChR2: n = 10 PCs from 4 cocultures, ChR2 + P/Q KD: n = 10 PCs from 4 cocultures; $P = 0.4450$, Mann-Whitney U test). Data are expressed as mean ± SEM.

Figure S3, related to Figure 3.

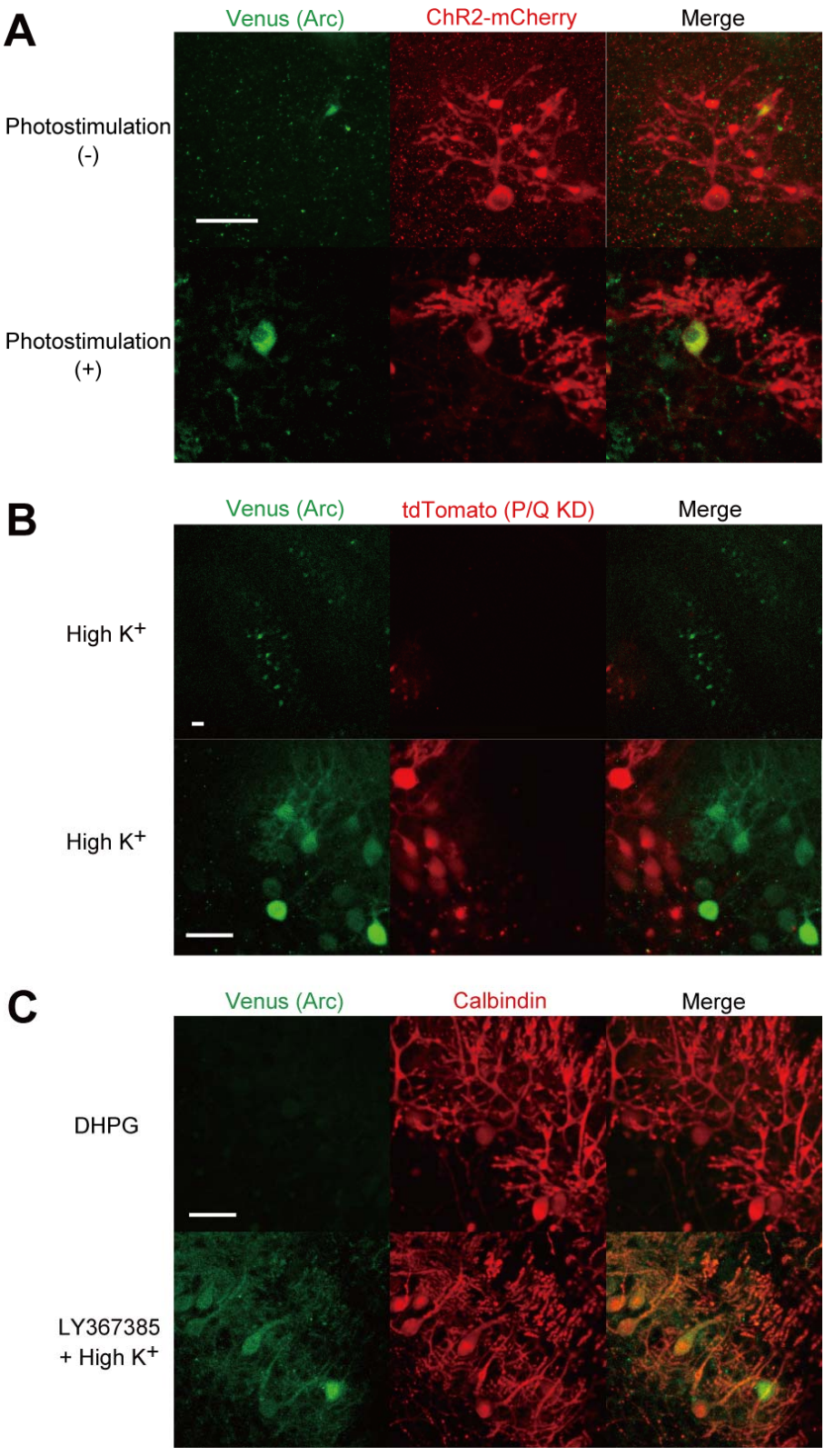

Figure S3, related to Figure 3.

P/Q-Type VDCCs Are Crucial for Activity-Dependent Expression of Arc in PCs

(A) Fluorescent labeling of Venus (Arc expression reporter, green) and ChR2-mCherry (red) in cocultured cerebellar slices derived from *Arc-pro-Venus-pest* transgenic mice. Blue light (1-s light exposure at 0.1 Hz) was applied for 6 h at 13 DIV. Scale bar, 50 μm.

(B) Fluorescent labeling for Venus (Arc expression reporter, green) and tdTomato (PCs infected with the P/Q-type VDCC knockdown virus, red) in cocultured cerebellar slices derived from *Arc-pro-Venus-pest* transgenic mice after incubation at 13 DIV for 5 h with high K^+ (60 mM)-containing culture medium. Scale bars, 50 μm. Note that cells infected with P/Q KD (in red, localized in the left of the upper (low magnification) and lower panels (high magnification)) have much less Venus fluorescence than the adjacent uninfected cells.

(C) Fluorescent labeling for Venus (Arc expression reporter, green) and calbindin (PCs, red) in cocultured cerebellar slices derived from *Arc-pro-Venus-pest* transgenic mice after incubation at 13 DIV for 5 h with DHPG (100 μM) or LY367385 (100 μM) + high K^+-containing culture medium. Scale bar, 50 μm.

Figure S4, related to Figures 4 and 5.

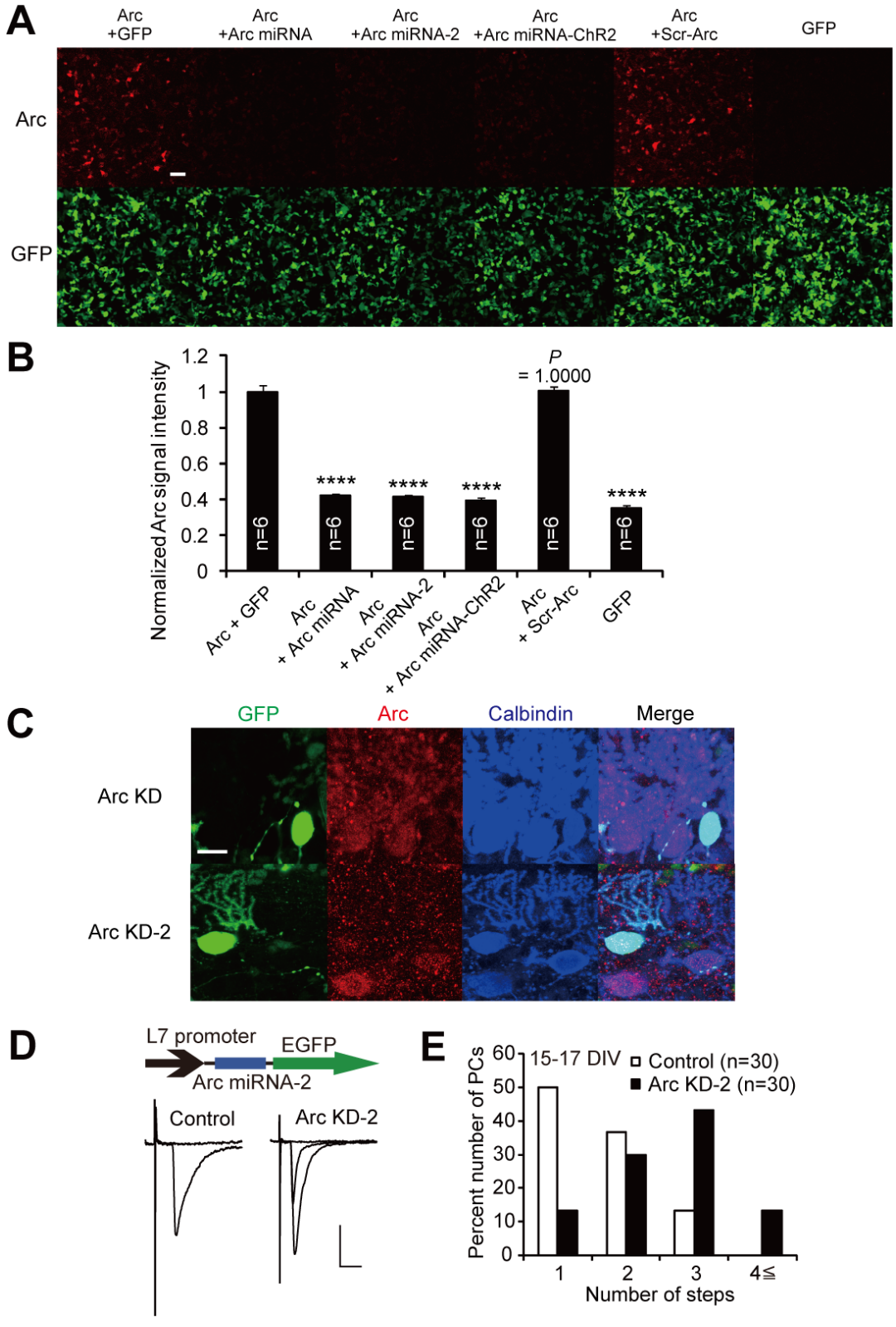

Figure S4, related to Figures 4 and 5.

Two Constructs of Arc miRNA Effectively Reduce Arc Expression

(A) Immunocytochemistry of HEK293T cells transfected with the indicated constructs using anti-Arc and anti-GFP antibodies. Scale bar, 100 μm.

(B) Summary graph showing Arc signal intensity normalized to the value of Arc + GFP. Six areas in the culture dish were examined for each group. Dunnett test, in comparison with Arc + GFP. ****P < 0.0001, P = 1.0000 for Arc + scrambled control Arc miRNA (Scr-Arc). Data are expressed as mean ± SEM.

(C) Triple immunolabeling for GFP (green), Arc (red) and calbindin (PCs, blue) in olivo-cerebellar cocultures with Arc knockdown ("Arc KD", upper) and Arc knockdown-2 ("Arc KD-2", lower) after treatment for 5 h with high K^+ (60 mM)-containing medium. Note that both Arc KD (upper) and Arc KD-2 (lower) in PCs suppressed Arc expression. Scale bar, 20 μm.

(D) Representative CF-EPSCs recorded at 15-17 DIV from a control uninfected PC (left) and a PC with Arc KD-2 (right). Scale bars, 10 ms and 1 nA. Holding potential, -30 mV.

(E) Frequency distribution histogram for the number of CFs innervating control PCs (open columns, n = 30 PCs) and PCs with Arc KD-2 (filled columns, n = 30 PCs) from 20 cocultures. Frequency distribution was significantly different between the two groups of PCs (P < 0.0001, Mann-Whitney U test).

Figure S5, related to Figure 6.

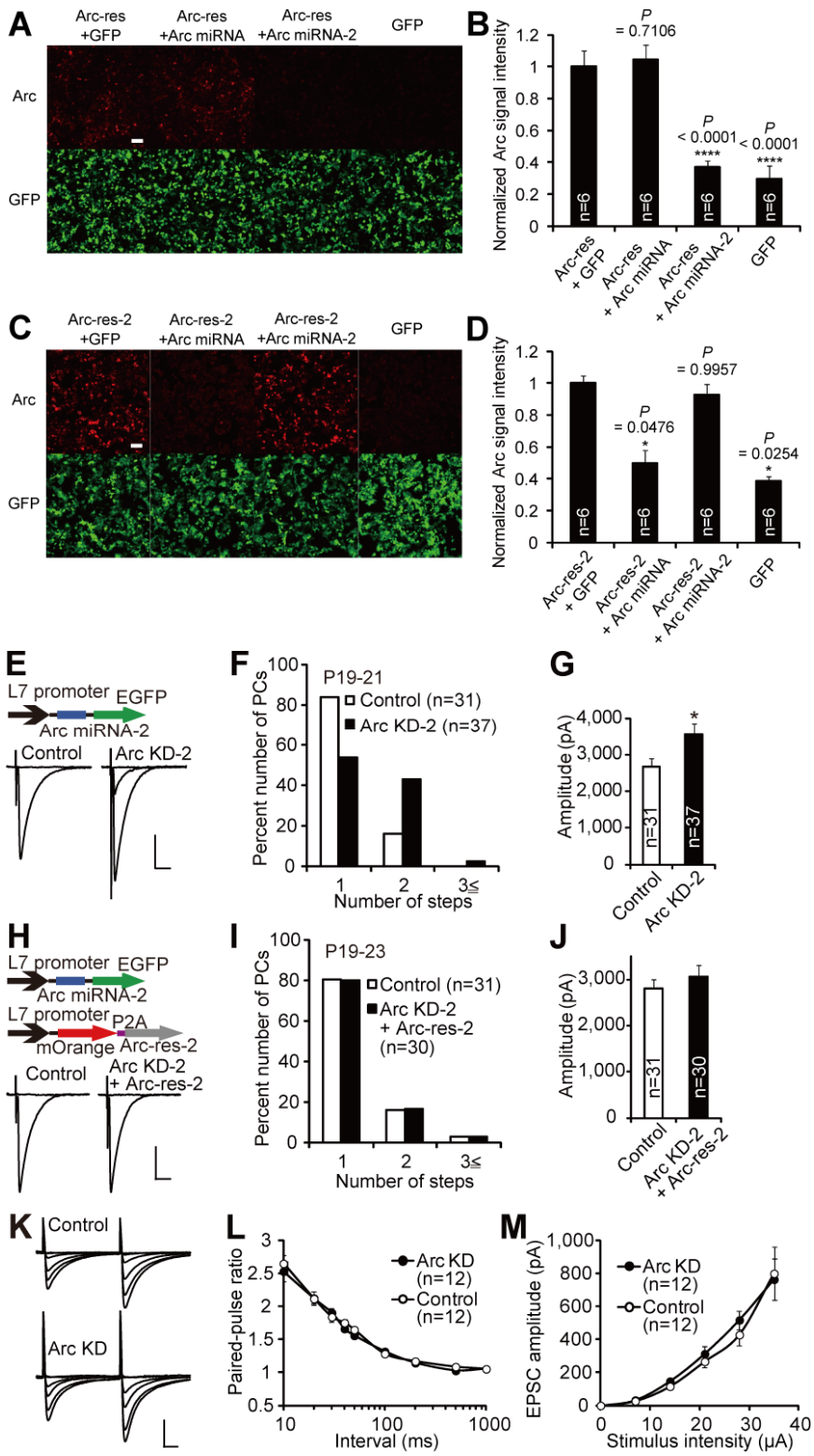

Figure S5, related to Figure 6.

Characterization of RNAi-Resistant Forms of Arc (A-D), Impaired CF Synapse Elimination in Arc Knockdown-2 PCs (E-J), and Normal Short-Term Plasticity and Normal Input-Output Relationship at PF-PC Synapses in Arc Knockdown PCs *in Vivo* (K-M)

(A) Immunocytochemistry of HEK293T cells transfected with the indicated constructs using anti-Arc and anti-GFP antibodies. Arc miRNA-resistant form of Arc (Arc-res) was not influenced by Arc miRNA but significantly suppressed by Arc miRNA-2. Scale bar, 100 μm.

(B) Summary graph showing Arc signal intensity normalized to the value of Arc-res + GFP. Six areas in the culture dish were examined for each group. Dunnett test, in comparison with Arc-res + GFP. P = 0.7106 for Arc-res + Arc miRNA, $P < 0.0001$ for Arc-res + Arc miRNA-2 and for GFP.

(C) The expression of Arc miRNA-2-resistant form of Arc (Arc-res-2) was not influenced by Arc miRNA-2 but significantly suppressed by Arc miRNA. Scale bar, 100 μm.

(D) Summary graph showing Arc signal intensity normalized to the value of Arc-res-2 + GFP. Six areas in the culture dish were examined for each group. Dunnett test, in comparison with Arc-res-2 + GFP. P = 0.9957 for Arc-res-2 + Arc miRNA-2, P = 0.0476 for Arc-res-2 + Arc miRNA and P = 0.0254 for GFP.

(E) Representative traces of CF-EPSCs recorded from a control uninfected PC (left) and a PC with Arc KD-2 (right). Lentivirus carrying Arc miRNA-2 was injected into the cerebellar vermis at P2-3, and CF-EPSCs were recorded from PCs in acute cerebellar slices prepared from 6 mice at P19-24.

(F) Frequency distribution histogram for the number of CFs innervating control PCs (open columns, n = 31 PCs) and PCs with Arc KD-2 (filled columns, n = 37 PCs). Frequency distribution was significantly different between the two groups of PCs (P = 0.0088, Mann-Whitney U test).

(G) Summary bar graph for the total amplitude of CF-EPSCs in control PCs (n = 31 PCs) and PCs with Arc KD-2 (n = 37 PCs). *P = 0.0488, Mann-Whitney U test.

(H) Representative traces of CF-EPSCs in an uninfected control PC (left) and a PC transfected with Arc KD-2 + Arc-res-2 (right). A mixture of lentiviral vectors carrying Arc KD-2 and Arc-res-2 was injected into the cerebellum at P2-3, and CF innervation patterns were examined in 5 mice at P19-23.

(I) Frequency distribution histogram for the number of CFs innervating control PCs (open columns, n = 31 PCs) and PCs transfected with Arc KD-2 + Arc-res-2 (filled columns, n = 30 PCs). No significant difference was detected between control and Arc KD-2 + Arc-res-2 (P = 0.9584, Mann-Whitney U test).

(J) Summary bar graph for the total amplitude of CF-EPSCs in control PCs (n = 31 PCs) and PCs transfected with Arc KD-2 + Arc-res-2 (n = 30 PCs). No significant difference was detected between control and Arc KD-2 + Arc-res-2 (P = 0.1833, Mann-Whitney U test).

(K) Specimen records of PF-EPSCs from a control (upper) and an Arc KD (lower) PC.

(L) Paired-pulse ratio of PF-EPSCs recorded from Arc KD (n = 12) and control (n = 12) PCs from 6 slices. There was no significant difference between the two groups of PCs (P = 0.3030, two-way ANOVA).

(M) Input-output relationship of PF-EPSCs recorded from Arc KD (n = 12) and control (n = 12) PCs from 6 slices. There was no significant difference between the two groups of PCs (P = 0.3910, two-way ANOVA).

Scale bars, 10 ms and 1 nA (E and H) and 10 ms and 500 pA (K). Holding potential, -10 mV (E-J) and -70 mV (K-M). In B, D, G, J, L and M, data are expressed as mean ± SEM.

Figure S6, related to Figure 7.

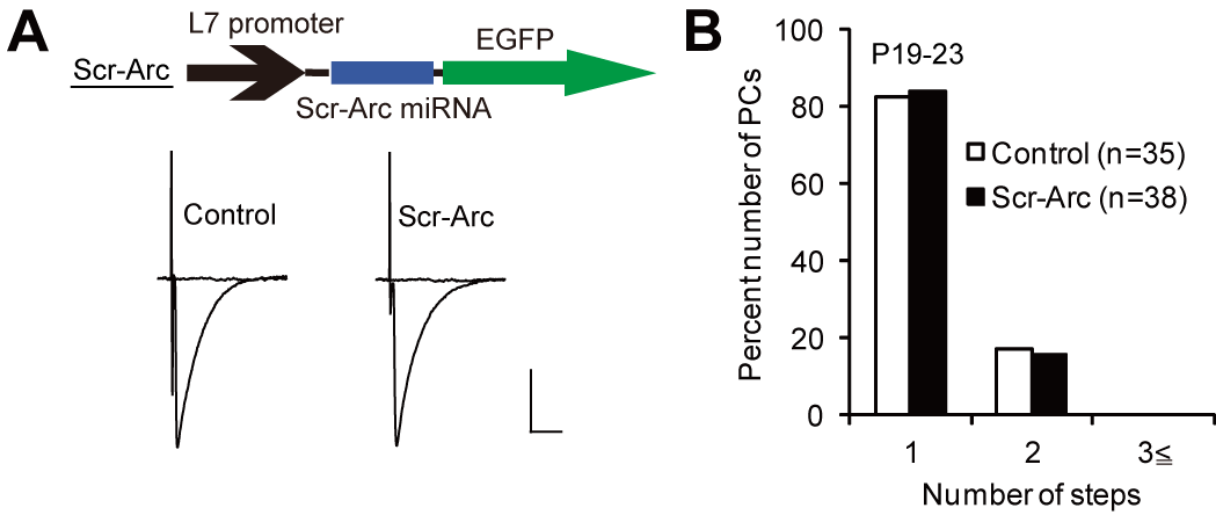

Figure S6, related to Figure 7.

CF Synapse Elimination Is Not Influenced by the Expression of Scrambled Control of Arc miRNA

(A) Specimen records of CF-EPSCs in a control (left, with 1 EPSC step) and a Scr-Arc (right, with 1 EPSC step) PC. Lentivirus encoding scrambled control of Arc miRNA (Scr-Arc) and EGFP was injected into the cerebellum at P2-3, and CF-EPSCs were recorded at P19-23 from 5 mice. Scale bars, 10 ms and 1 nA. Holding potential, -10 mV.

(B) Frequency distribution histogram for the number of CFs innervating control (open columns, n = 35) and Scr-Arc (filled columns, n = 38) PCs. There was no significant difference in frequency distribution between the two groups of PCs (P = 0.8770, Mann-Whitney U test).

Figure S7, related to Figure 8.

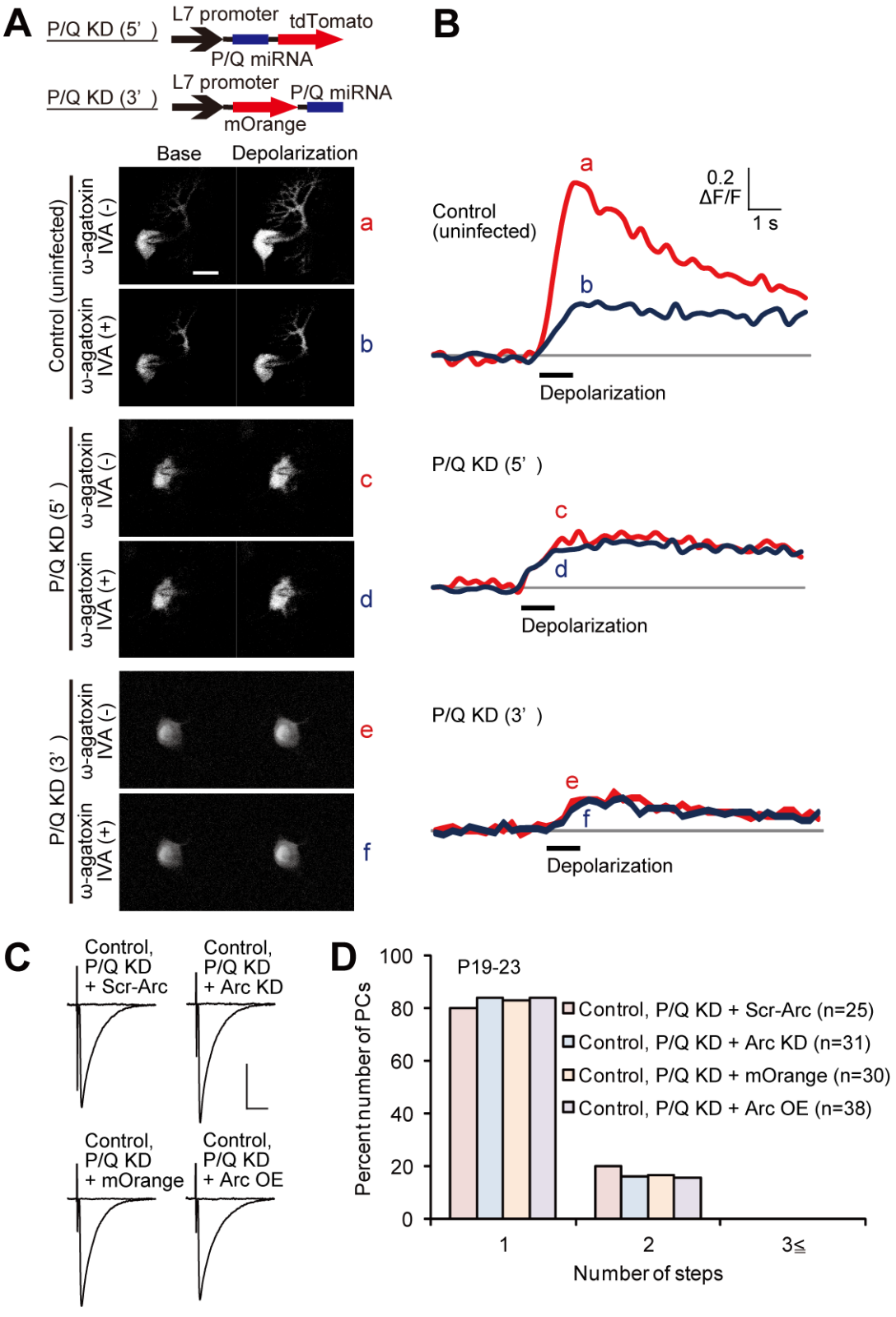

Figure S7, related to Figure 8.

Expression of P/Q miRNA in PCs *in Vivo* at P2 Suppresses the Function of P/Q-Type VDCCs at P9

(A) P/Q miRNA and a fluorescent protein, tdTomato or mOrange, were driven by L7 promoter for PC-specific P/Q knockdown (P/Q KD). P/Q KD (5') and P/Q KD (3') indicate that P/Q miRNA is located at the 5'-side of tdTomato and 3'-side of mOrange, respectively. Lentivirus was injected in the mouse cerebellum at P2, and acute cerebellar slices were prepared at P9. PCs in the slices were loaded with a Ca^{2+} indicator dye (Oregon Green BAPTA-1, 0.1 mM) through patch pipettes. Ca^{2+} signals were measured from the soma before and after direct depolarization from -70 mV to 0 mV for 1 s, before and after application of ω-agatoxin IVA (0.4 μM). Scale bar, 20 μm.

(B) Representative Ca^{2+}-dependent fluorescent signals from a control (uninfected, top), a P/Q KD (5') (middle) and a P/Q KD (3') (bottom) PC. Ca^{2+} influx after depolarization was smaller in both P/Q KD (5') and P/Q KD (3') PCs. Bath-applied ω-agatoxin IVA robustly decreased Ca^{2+} transients in the control PC, while ω-agatoxin IVA caused little change in both P/Q KD (5') and P/Q KD (3') PCs.

(C) Specimen records of CF-EPSCs in control (uninfected) PCs for P/Q KD + Scr-Arc, P/Q KD + Arc KD, P/Q KD + mOrange and P/Q KD + Arc overexpression (Arc OE). All the PCs had single EPSC steps. Scale bars, 10 ms and 1 nA. Holding potential, -10 mV.

(D) Frequency distribution histogram for the number of CFs innervating control PCs for P/Q KD + Scr-Arc (n = 25), P/Q KD + Arc KD (n = 31), P/Q KD + mOrange (n = 30) and P/Q KD + Arc OE (n = 38). There was no significant difference in frequency distribution among the four groups of PCs (P = 0.9749, Kruskal-Wallis test).

SUPPLEMENTAL TABLES

Table S1, related to Figures 1 and 4.

	10-90% rise time, ms	Total amplitude, pA	Disparity index	Disparity ratio
ChR2	0.8 ± 0.2 (33)	1683 ± 1037 (33)	0.47 ± 0.33 (29)	0.55 ± 0.27 (29)
Control	0.8 ± 0.2 (37)	2118 ± 1500 (37)	0.64 ± 0.28 (21)	0.41 ± 0.20 (21)
P/Q KD	0.8 ± 0.2 (26)	2332 ± 1372 (26)	0.52 ± 0.25 (26)	0.51 ± 0.19 (26)
Control	0.7 ± 0.2 (24)	2170 ± 1590 (24)	0.42 ± 0.22 (20)	0.58 ± 0.22 (20)
Arc KD	0.7 ± 0.1 (26)	**3881 ± 2514 (26)	0.61 ± 0.31 (26)	0.44 ± 0.22 (26)
Control	0.8 ± 0.1 (20)	2448 ± 1585 (20)	0.52 ± 0.26 (20)	0.50 ± 0.21 (20)
Arc KD-2	0.8 ± 0.2 (25)	3321 ± 2699 (25)	0.48 ± 0.20 (25)	0.52 ± 0.16 (25)
Control	0.7 ± 0.3 (19)	2423 ± 1649 (19)	0.50 ± 0.22 (15)	0.50 ± 0.17 (15)

***P* = 0.0094

Table S1, related to Figures 1 and 4.

Kinetics and Disparity Parameters of CF-EPSCs in Cocultures

Data are expressed as mean ± SD. For 10-90% rise time, the first step of multiple CF-EPSCs was used for analysis. The numbers of PCs analyzed are indicated in parentheses. ***P* = 0.0094 (Mann-Whiteny U test, comparison with the values of the corresponding controls). Amplitudes are measured at Vh = -30 mV.

Table S2, related to Figure 6.

	Disparity index	Disparity ratio	Paired-pulse ratio (interval = 50 ms)
Arc KD	1.00 ± 0.35 (28)	0.21 ± 0.20 (28)	0.74 ± 0.06 (10)
Control	0.77 ± 0.49 (8)	0.36 ± 0.34 (8)	0.77 ± 0.04 (10)
Arc KD-2	0.91 ± 0.36 (17)	0.26 ± 0.23 (17)	0.69 ± 0.10 (10)
Control	0.60 ± 0.48 (5)	0.47 ± 0.34 (5)	0.72 ± 0.03 (10)

Table S2, related to Figure 6.

Disparity Parameters and Paired-Pulse Ratio of CF-EPSCs from Arc Knockdown PCs *in Vivo*

Data are expressed as mean ± SD. The numbers of PCs analyzed are indicated in parentheses.

Table S3, related to Figure 6.

	CF group	10-90% rise time, ms	Decay time constant, ms	Amplitude, pA	n
Arc KD	CF-mono	0.5 ± 0.1	*6.8 ± 2.7	**3235 ± 1090	30
	CF-multi-S	0.5 ± 0.1	6.5 ± 2.4	2600 ± 1008	27
	CF-multi-W	0.5 ± 0.2	4.1 ± 2.7	555 ± 670	20
Control	CF-mono	0.5 ± 0.1	8.5 ± 3.2	2540 ± 1028	40
	CF-multi-S	0.5 ± 0.1	7.0 ± 2.2	2093 ± 634	8
	CF-multi-W	0.5 ± 0.1	6.4 ± 1.2	658 ± 584	8
Arc KD-2	CF-mono	0.5 ± 0.1	7.5 ± 1.2	3096 ± 1561	21
	CF-multi-S	0.5 ± 0.1	6.6 ± 1.9	3086 ± 1580	16
	CF-multi-W	0.5 ± 0.2	5.7 ± 2.3	607 ± 433	17
Control	CF-mono	0.5 ± 0.1	7.3 ± 1.0	2506 ± 1152	26
	CF-multi-S	0.5 ± 0.1	6.6 ± 0.2	2421 ± 1107	5
	CF-multi-W	0.5 ± 0.2	5.8 ± 3.3	1084 ± 860	5

*P = 0.0163

**P = 0.0030

Table S3, related to Figure 6.

Kinetics of CF-EPSCs from Arc Knockdown PCs *in Vivo*

Data are expressed as mean ± SD. CF-EPSCs are divided into three groups, namely CF-EPSCs from mono-innervated PCs (CF-mono), the largest CF-EPSCs in individual multiply innervated PCs (CF-multi-S), and other smaller CF-EPSCs in individual multiply innervated PCs (CF-multi-W). *P = 0.0163, **P = 0.0030 (Mann-Whitney U test, comparison with the values of the corresponding controls). Amplitudes are measured at Vh = -10 mV.

SUPPLEMENTAL TEXT

The Effect of the 2-Day Excitation of PCs on Electrophysiological Properties of CFs, PFs and PCs

We examined the effect of the 2-day excitation of PCs on electrophysiological properties of CFs and PCs. The 10-90% rise time and the amplitude of CF-EPSCs were similar between photostimulated and control PCs (Table S1). We then checked whether selective strengthening of a single CF among multiple CFs was influenced by photostimulation. We calculated the disparity ratio and disparity index for each multiply innervated PCs, which have been used for estimating relative strengths of CF inputs (Hashimoto and Kano, 2003). These values were similar between photostimulated and control PCs (Table S1). Input resistance was not significantly different between photostimulated and control PCs (photostimulated: 29.5 ± 2.3 MΩ, 10 PCs; control: 27.2 ± 2.4 MΩ, 10 PCs; 6 cocultures; $P = 0.5955$, Mann-Whitney U test).

Synapse formation on PCs from parallel fibers (PFs), the other excitatory inputs to PCs, is known to influence CF synapse elimination (Hashimoto et al., 2009). The input-output curves of PF-mediated EPSCs (PF-EPSCs) in terms of stimulus strength were similar between photostimulated and control PCs (Figures S1F and S1G; $P = 0.7800$, two-way ANOVA), suggesting that the formation and function of PF-PC synapses were normal in photostimulated PCs.

Knockdown of the P/Q-Type VDCC Impairs CF Synapse Elimination in Cocultures

To inhibit the function of P/Q-type VDCCs in PCs, we constructed lentiviruses containing engineered miRNA targeting the P/Q-type VDCC (P/Q miRNA) and a gene encoding a fluorescent protein under the control of L7 promoter (Figure S2A). We confirmed the effectiveness of the P/Q miRNA by measuring the fraction of depolarization-induced Ca^{2+} transients mediated by P/Q-type VDCCs (Figures S2A-S2C; $P < 0.0001$, Student's t test). We found that a significantly higher number of CFs innervated P/Q miRNA-expressing (P/Q knockdown) PCs at 15-17 DIV when compared to virus-uninfected control PCs (Figures S2D and S2E; $P = 0.0017$, Mann-Whitney U test). These results demonstrate that P/Q-type VDCCs are required for CF synapse elimination in cocultures as well as *in vivo* (Hashimoto et al., 2011; Miyazaki et al., 2004).

Specificity of the Effect of Arc Knockdown on CF Synapse Elimination in Cocultures

To verify the specificity of the effect of Arc knockdown on CF synapse elimination, we constructed lentiviruses expressing Arc miRNA-2, another miRNA construct directed against Arc which does not overlap with Arc miRNA, together with EGFP under the control of L7 promoter. Introduction of Arc miRNA-2 reduced Arc expression as robustly as Arc miRNA to background (only-GFP-expressing) level in Arc-overexpressed HEK293T cells (Figures S4A and S4B; $P < 0.0001$, Dunnett test). Arc miRNA-2 also reduced the activity-dependent expression of Arc in PCs in cocultures (Figure S4C).

We found that 57% of PCs expressing Arc miRNA-2 (Arc knockdown-2 PCs) were innervated by three or more CFs whereas 13% of uninfected (control) PCs were innervated in the same way at 15-17 DIV (Figures S4D and S4E). The frequency distribution histogram clearly shows that PCs with Arc knockdown-2 were innervated by a significantly higher number of CFs than control PCs (Figure S4E, $P < 0.0001$, Mann-Whitney U test). Thus, two distinct nonoverlapping miRNA constructs directed against Arc (Arc miRNA and Arc miRNA-2) have similar effects on CF synapse elimination, demonstrating that Arc is involved in CF synapse elimination.

The 10-90% rise time of CF-mediated excitatory postsynaptic currents (CF-EPSCs) was similar between control and Arc knockdown-2 PCs. There was a tendency for the total amplitude of CF-EPSCs to be larger in Arc knockdown-2 PCs than in control PCs, although the difference did not reach a statistically significant level (Table S1; $P = 0.1220$, Mann-Whitney U test). We then checked whether selective strengthening of a single CF among multiple CFs was influenced by Arc knockdown-2. We calculated the disparity ratio and disparity index for each multiply innervated PCs (see Supplemental Experimental Procedures) (Hashimoto and Kano, 2003). We found that both parameters were similar between Arc knockdown-2 PCs and control PCs (Table S1).

Specificity of the Effect of Arc Knockdown on CF Synapse Elimination *in Vivo*

To further confirm the specificity of the effect of Arc knockdown on CF synapse elimination *in vivo*, we examined CF innervation patterns in Arc miRNA-2 expressing (Arc knockdown-2) and uninfected (control) PCs in acute cerebellar slices obtained from P19-21. We found that PCs with Arc knockdown-2 were innervated by a significantly higher number of CFs than control PCs (Figures S5E and S5F; $P = 0.0088$, Mann-Whitney U test), indicating that the regression of surplus CFs was impaired in Arc knockdown-2 PCs. To exclude the possibility of off-target effect of Arc miRNA-2, we constructed lentiviruses that encode an Arc miRNA-2-resistant form of Arc (Arc-res-2) together with mOrange. Arc-res-2 was shown to be refractory to Arc miRNA-2 in HEK293T cells (Figures S5C and S5D). We injected the mixture of lentiviruses carrying Arc knockdown-2 and Arc-res-2 into the mouse cerebellum and found that most infected PCs exhibited expression of both EGFP (Arc knockdown-2) and mOrange (Arc-res-2). There was no significant difference in CF innervation patterns between PCs with Arc knockdown-2 + Arc-res-2 and uninfected (control) PCs (Figures S5H and S5I; $P = 0.9584$, Mann-Whitney U test). This result clearly indicates that the impairment of CF synapse elimination in Arc knockdown-2 PCs was rescued by exogenous expression of Arc-res-2 in PCs. Thus, we have demonstrated that two distinct nonoverlapping miRNA constructs targeting Arc (Arc miRNA and Arc miRNA-2) have exactly the same effects on CF synapse elimination, which confirms a pivotal role of Arc in CF synapse elimination *in vivo*.

We examined the effect of Arc knockdown-2 on other parameters of CF-PC synaptic transmission. The total amplitude of CF-EPSCs was significantly larger in Arc knockdown-2 PCs than in control PCs (Figure S5G; $P = 0.0488$, Mann-Whitney U test), which was compatible with the result of Arc

knockdown in cocultures (Table S1) and *in vivo* (Figure 6D). The larger amplitude of CF-EPSCs in Arc knockdown-2 PCs was restored to the normal level when Arc-res-2 was simultaneously expressed, indicating that the larger amplitude of EPSC was also attributable to Arc knockdown-2 (Figure S5J; P = 0.1833, Mann-Whitney U test). The paired-pulse ratio of CF-EPSCs (Table S2; P = 0.2530, Mann-Whitney U test), the disparity index and disparity ratio (Table S2; disparity index: P = 0.2536, disparity ratio: P = 0.1961, Mann-Whitney U test), and the 10-90% rise time of CF-EPSCs (Table S3) were similar between Arc knockdown-2 PCs and control PCs. These results indicate that Arc knockdown-2 in PCs did not affect basic properties of CF-PC synapses or functional differentiation of CF inputs.

Taken together, these results demonstrate that both Arc miRNA and Arc miRNA-2 have essentially the same effects on development of CF synapses *in vivo* as well as in cocultures, and clearly indicate that Arc is crucial for CF synapse elimination. Thus, we explored further mechanisms of CF synapse elimination by using Arc miRNA in Figures 7 and 8.

SUPPLEMENTAL EXPERIMENTAL PROCEDURES

Animals

To generate lines of transgenic mice harboring the *Arc-pro-Venus-pest* transgene, an enhanced version of YFP (Venus) cDNA (Nagai et al., 2002) was subcloned into a plasmid containing the 7-kb regulatory region of the *Arc* gene (Kawashima et al., 2009). The Venus reporter was destabilized by adding a PEST signal sequence from the mouse ornithine decarboxylase with D433A/D434A mutations to accelerate its degradation rate (Li et al., 1998). The *Arc-pro-Venus-pest* transgene was microinjected into the pronucleus of fertilized mouse eggs to produce founder mice. Detailed characterization of *Arc-pro-Venus-pest* transgenic mice will be described elsewhere (H.O. and H.B., in preparation). Genomic integration of the transgene and reporter expression were analyzed by PCR, Southern blotting, Western blotting and histological assays.

Organotypic Cocultures of the Cerebellum and Medulla Oblongata

The olivo-cerebellar cocultures were prepared as described previously (Uesaka et al., 2012). In brief, the ventral medial portion of the medulla containing inferior olivary neurons was dissected from rat embryo at embryonic day 15. Cerebellar slices of 250 μm thickness were dissected from the vermis of P10 mice. A block of the medulla was plated at the ventricular side of the cerebellar slice on a membrane filter (Millicell-CM PICMORG50, MILLIPORE), which was coated with rat tail collagen. The culture medium consisted of 50% MEM, 25% horse serum (STEMCELL), 2.5% Hanks' balanced salts solution (Nacalai Tesque), 3 mM GlutaMAX (Gibco), 10 μM Mifepristone (Ru486, TOCRIS), 5 mg/ml glucose and 2% B27 supplements (Gibco). These cultures were maintained at 37 ^{o}C in an environment of humidified 95% air and 5% CO_2. One-half of the culture medium was exchanged with fresh medium every other day.

Preparation of Viral Vector Constructs

VSV-G pseudotyped lentiviral vectors (pCL20c) (Hanawa et al., 2002) were used in this study. The vectors were designed for PC-specific expression under the control of a truncated L7 promoter (pCL20c-L7) (Sawada et al., 2010). ChR2-EYFP and ChR2-mCherry was PCR'd out from pLenti-CaMKIIa-hChR2(H134R)-EYFP/mCherry-WPRE (Boyden et al., 2005) and subcloned into pCL20c-L7. Arc cDNA was obtained by RT-PCR using cDNA library from P16 mouse cerebellum and subcloned into pCL20c-L7. QuikChange lightning site-directed mutagenesis kit (Agilent Technologies) was used to generate RNAi-resistant form of Arc (Arc-res and Arc-res-2), which harbors sense mutations (no alteration of amino acid codons) at the recognition site of Arc miRNA and Arc miRNA-2, respectively. The following sequences were used to generate Arc-res and Arc-res-2:
5'-CGGGGTGGGCCGGCCGCTAAGCCTAACGTCATTCTCCAGATTGGTAAGTGCCGA-3' and
5'-TCGGCACTTACCAATCTGGAGAATGACGTTAGGCTTAGCGGCCGGCCCACCCCG-3' for Arc-res;
5'-CGGAGGACCCACCGGCACCTCCTGACAGAGGTCTCTAAGCAGGTGGAGCGAGA-3' and
5'-TCTCGCTCCACCTGCTTAGAGACCTCTGTCAGGAGGTGCCGGTGGGTCCTCCG-3' for Arc-res-2. mOrange and Arc/Arc-res/Arc-res-2 were linked in-frame, interposed by picornavirus "self-cleaving" P2A peptide sequence to enable efficient bicistronic expression (Szymczak et al., 2004) and then subcloned into pCL20c-L7.

Unlike shRNA, miRNA can be driven by cell-type-specific RNA-polymerase-II-based promoter such as L7 (Amarzguioui et al., 2005). Engineered miRNA targeting a gene of interest and a gene encoding a fluorescent protein or any other protein can be driven by a single cell-type-specific promoter through co-cistronic expression. Furthermore, engineered miRNA can be tandemly inserted into either 5'- or 3'-side of a gene (Hamacher-Brady et al., 2006; Uesaka et al., 2012). Taking advantage of these properties of miRNA, we carried out vector-based RNAi analysis using BLOCK-iT Pol II miR RNAi expression vector kit (Invitrogen). The miRNA constructs were produced by PCR amplification of miRNA region in BLOCK-iT Pol II miR RNAi expression vector followed by subcloning into pCL20c-L7 at 5'- or 3'-side of a fluorescent protein or ChR2 as indicated in the figures. Engineered oligonucleotides for miRNAs with the following sequences
(5'-TGCTGTTCCAATGAAGTATGGTTCCGGTTTTGGCCACTGACTGACCGGAACCACTTCATTGGAA
-3' and
5'-CCTGTTCCAATGAAGTGGTTCCGGTCAGTCAGTGGCCAAAACCGGAACCATACTTCATTGGAAC-
3' for P/Q miRNA;
5'-TGCTGTGCAGGATCACATTGGGTTTGGTTTTGGCCACTGACTGACCAAACCCAGTGATCCTGCA-
3' and
5'-CCTGTGCAGGATCACTGGGTTTGGTCAGTCAGTGGCCAAAACCAAACCCAATGTGATCCTGCAC
-3' for Arc miRNA;
5'-TGCTGTGGACACTTCGGTCAACAGATGTTTTGGCCACTGACTGACATCTGTTGCGAAGTGTCCA-
3' and

5’-CCTGTGGACACTTCGCAACAGATGTCAGTCAGTGGCCAAAACATCTGTTGACCGAAGTGTCCAC-3’ for Arc miRNA-2;
5’-TGCTGGAGTACTCTAGTGTCGTAGGTGTTTTGGCCACTGACTGACACCTACGACTAGAGTACTC-3’ and
5’-CCTGGAGTACTCTAGTCGTAGGTGTCAGTCAGTGGCCAAAACACCTACGACACTAGAGTACTCC-3’ for scrambled control Arc miRNA) were designed against the mouse α1A subunit of the P/Q-type VDCC (21 nucleotides from 694th to 714th in the coding region) or Arc mRNA (Arc miRNA: 69th-89th, Arc miRNA-2: 143rd-163rd nucleotides in the coding region) sequence following the BLOCK-iT Pol II miR RNAi Expression Vector kit guidelines (Invitrogen). Note that Arc miRNA and Arc miRNA-2 are nonoverlapping each other. The sequence for scrambled control Arc miRNA (Scr-Arc) was designed by shuffling the sequence of recognition region of Arc miRNA. We confirmed the scrambled sequence has no target gene by BLAST search. All the constructs were verified by DNA sequencing.

Virus Preparation

The virus vector was produced by cotransfection of sub-confluent HEK293T cells with a mixture of two packaging plasmids (7 μg of psPAX2 and 3 μg of pCAG-VSVG) and one lentivirus vector (10 μg of pCL20c-L7) using a calcium phosphate precipitation method (Torashima et al., 2006). Sixteen hours after the transfection, culture medium was exchanged with a fresh medium. The medium containing vector particles was harvested 40 h after the transfection. The medium samples were filtered through 0.22 μm membranes and centrifuged at 120,000 g for 90 min. The virus samples were finally suspended in 30 μl of culture medium for *in vitro* and PBS for *in vivo* experiments to be stored at 4 °C.

Virus Infection

For *in vitro* virus infection, cultured PCs were infected at 0 or 1 day *in vitro* (DIV) by adding 0.5 μl (0.2-1 x 10^5 TU) of viral solution per coculture directly on the slices with 33-gauge needle microsyringe (ITO CORPORATION). For *in vivo* virus infection, C57BL/6 mice at P2-3 were used. Each mouse was anesthetized by inhalation of 1-2% isoflurane. The mouse was mounted on a head-holding device (Narishige Int.) in conjunction with ear spacers (Narishige Int.). A midline sagittal incision was made and the cranium over the cerebellar vermis was exposed. A burr hole was drilled at the midline, 0.5 mm caudal from the transverse occipital suture (Mendosal suture). The tip of a 33-gauge Hamilton syringe attached to a micropump (UltramicroPump II; World Precision Instruments (WPI)) was placed on the surface of the cerebellar vermis (lobule 6). An aliquot of 3 μl (5 x 10^5 TU) of viral solution was injected at a rate of 180 nl/min using a microprocessor-based controller (Micro 4; WPI). The syringe was left in place for an additional 2 min before it was withdrawn. The scalp was then sutured and the mouse was returned to its home cage.

Photostimulation

For electrophysiological recordings, cocultures were illuminated with blue LEDs (OSUB5161P, 470 nm; OptoSupply Limited; maximal power density is 0.34 mW/mm^2 measured 2 cm from the source) or mercury lump using GFP filter set (USH1030-L; Olympus; 0.66 mW/mm^2 measured 2 cm from the source). For long-term photostimulation in a humidified incubator (37°C, 5% CO_2), we placed the blue LEDs onto culture dishes (the distance between the LEDs and cocultures was 2 cm), controlled by a Master-8 stimulator (A.M.P.I.).

Electrophysiological Recordings from PCs in Cocultures

For recordings from PCs in cocultures, most part of the medullary explant was cut from the coculture to reduce responses elicited by spontaneous firing of inferior olivary neurons. The cocultures were recovered for at least 30 min at room temperature in a reservoir chamber bathed with the solution with the following composition (in mM): 125 NaCl, 2.5 KCl, 2 $CaCl_2$, 1 $MgSO_4$, 1.25 NaH_2PO_4, 26 $NaHCO_3$, and 20 glucose bubbled with 95% O_2 and 5% CO_2. Cocultures were transferred to a recording chamber on the stage of an Olympus BX51WI microscope (Olympus). The recording chamber was continuously perfused with oxygenated bath solution at 32 ^oC, supplemented with picrotoxin (TOCRIS; 0.1 mM) to block inhibitory synaptic transmission. Whole-cell and cell-attached recordings were made from visually identified or fluorescent protein positive PCs using an upright fluorescence microscope. The resistance of patch pipettes was 2–4 MΩ when filled with one of the following internal solutions containing (in mM): (1) 60 CsCl, 10 Cs D-gluconate, 20 TEA-Cl, 20 BAPTA, 4 $MgCl_2$, 4 ATP, 0.4 GTP, and 30 HEPES (pH 7.3, adjusted with CsOH) for voltage-clamp recordings; (2) 130 K D-gluconate, 6 KCl, 10 NaCl, 10 HEPES, 0.16 $CaCl_2$, 2 $MgCl_2$, 0.5 EGTA, 4 ATP, and 0.4 GTP (pH 7.3, adjusted with KOH) for current-clamp recordings; (3) 125 NaCl, 2.5 KCl, 10 HEPES, 2 $CaCl_2$, 1 $MgSO_4$ (pH 7.3, adjusted with NaOH) for cell-attached recordings. The pipette access resistance was compensated by 70%. All electrophysiological recordings were made with an EPC-9 patch clamp amplifier (HEKA Elektronik). The signals were filtered at 2 kHz and digitized at 20 kHz. On-line data acquisition and off-line data analysis were performed using PULSE software (HEKA). Holding potential was -30 mV for CF-EPSCs and -70 mV for PF-EPSCs (corrected for liquid junction potential). When the number of CF-EPSC steps was examined, R-3-(2-carboxypiperazin-4-yl)-propyl-1-phosphonic (R-CPP, TOCRIS; 5 μM) was added to block NMDA receptor-mediated spontaneous excitatory synaptic transmission onto cerebellar granule cells, and thus to suppress PF-mediated spontaneous excitatory inputs to PCs. Since CF-EPSCs are elicited in an all-or-none manner and display paired-pulse depression, they can easily be distinguished from PF-mediated EPSCs that exhibit paired-pulse fascilitation (Konnerth et al., 1990). To stimulate CFs, square voltage pulses (duration, 0.1 ms; amplitude, 0-90 V) were applied between two of the eight tungsten electrodes (3.5-4.5 MΩ, Catalog #UEWMGCSEKNNM, FHC) placed in the remaining portion of medullary explants. Electrical pulses were applied between all possible combinations of two electrodes. More than one discrete steps of CF-EPSC were elicited in multiply innervated PCs when the stimulus

intensity was gradually increased. Since CF-EPSCs are elicited in an all-or-none manner, the number of CFs innervating the recorded PC was estimated by the number of discrete CF-EPSC steps (Uesaka et al., 2012). To record PF-EPSCs, glass pipettes filled with the bathing solution were used to apply square pulses for focal stimulation (duration, 0.1 ms; amplitude, 0-35 μA). PFs were stimulated in the molecular layer at a distance of 50-100 μm from the PC soma.

Electrophysiological Recordings from PCs in Acute Cerebellar Slices

Parasagittal cerebellar slices (250 μm) were prepared from mice at P11-26 as described (Hashimoto and Kano, 2003). Bathing and intracellular solutions were the same as those used for recording from cocultures. The recording chamber was continuously perfused with the oxygenated bath solution supplemented with picrotoxin (0.1 mM). Holding potential was -10 mV for CF-EPSCs and -70 mV for PF-EPSCs (corrected for liquid junction potential). To record CF-EPSCs, stimuli (duration, 0.1 ms; amplitude, 0-90 V) were applied at 0.2 Hz through a patch pipette filled with normal external solution. CFs were stimulated in the granule cell layer 20-100 μm away from the PC soma. For each PC, the pipette for CF stimulation was moved systematically by about 20 μm step around the PC soma and the stimulus intensity was increased gradually from 0 V to about 90 V at each stimulation site. The number of CFs innervating the recorded PC was estimated by the number of discrete CF-EPSC steps as previously described (Hashimoto and Kano, 2003; Hashimoto et al., 2009).

Quantification of Disparity in Multiple CF-EPSCs

To quantify the disparity in multiple CF-EPSCs recorded in a given PC, we calculated the disparity index and disparity ratio for each PC as indicated below (Hashimoto and Kano, 2003). The amplitudes of individual CF-EPSCs in a given multiply-innervated PC were measured and they were numbered in the order of their amplitudes (A_1, A_2, $\cdots A_i$, $\cdots A_N$, $N \geq 2$; N is the number of CFs innervating a given PC. A_i is the EPSC amplitude for the CF_i recorded at the same holding potential. A_N represents the largest CF-EPSC). Parameters were represented by the following formulas.

Disparity Index = $\dfrac{S.D.}{M}$

$M = \dfrac{1}{N}\sum_{i=1}^{N} A_i$

$S.D. = \sqrt{\dfrac{1}{N-1}\sum_{i=1}^{N}\left(A_i - M\right)^2}$

Disparity Ratio = $\dfrac{\sum_{i=1}^{N-1}\dfrac{A_i}{A_N}}{N-1}$

The disparity index is the coefficient of variation for all CF-EPSC amplitudes recorded in a given PC. Hence, if CF-EPSCs are variable in size, the value will be large. On the other hand, the disparity ratio represents the average of the inverse proportion of the strongest CF-EPSC amplitude to each of the other weaker CF-EPSCs. Therefore, if the differences between A_N and the amplitudes of the other smaller CF-EPSCs are large, the disparity ratio will be small.

Ca^{2+} Imaging

PCs were loaded for at least 30 min with a Ca^{2+} indicator (Oregon Green 488 BAPTA-1, Molecular Probes; 0.2 mM for cultured PCs, 0.1 mM for PCs in acute slices) through patch pipette filled with an intracellular solution composed of (in mM) 130 K D-gluconate, 10 KCl, 10 NaCl, 0.5 EGTA, 10 HEPES, 4 ATP and 0.4 GTP (pH 7.3, adjusted with KOH). Fluorescence images were acquired by using a confocal laser-scanning microscope (Fluoview FV300, Olympus) before and after direct 1-s depolarization to 0 mV from -70 mV, before and 5 min after application of the P/Q-type VDCC blocker (ω-agatoxin IVA, Peptide Institute; 0.4 μM) (Hashimoto et al., 2011). The Ca^{2+}-dependent fluorescence signals from the PC soma were background corrected and expressed as increases in fluorescence divided by the prestimulus fluorescence values (ΔF/F) using the Image J software (http://rsbweb.nih.gov/ij/).

Elevation of Arc Expression in Cocultures

Cocultures of cerebellar slices derived from *Arc-pro-Venus-pest* transgenic mice and medullary explants were treated at 13 DIV with culture medium containing high K^+ (60 mM) or an mGluR1 agonist ((RS)-DHPG, TOCRIS; 100 μM) for 5 h. A P/Q-type VDCC blocker (ω-agatoxin IVA, Peptide Institute; 0.4 μM) or an mGluR1 antagonist (LY367385, TOCRIS; 100 μM) was applied 3 min before the high K^+ treatment. After the treatments, cocultures were fixed with 2.5% or 4% paraformaldehyde in 0.1 M phosphate buffer for 30 min followed by permeabilization with 1% Triton X-100 for 1 h. Nonspecific binding of antibodies was blocked with 5% donkey serum (Jackson ImmunoResearch Laboratories) in PBS. Then the rat anti-GFP antibody (Nacalai Tesque; 1/1000) or rabbit anti-Arc antibody (produced in Bito lab; OP-1, 1/1000) (Okuno et al., 2012) to visualize Arc expression and the mouse antibody against calbindinD28K (Sigma; 1/3000) to label PCs were incubated at 4°C. After incubation with secondary antibodies (anti-rat Alexa Fluor488 antibody, Molecular Probes, 1/300; anti-rabbit Alexa Fluor488 antibody, Molecular Probes, 1/300; anti-mouse Cy3 antibody, Jackson, 1/400), the immunolabeled sections were washed with PBS and examined with a confocal laser scanning microscope (LSM 510, Zeiss).

Immunohistochemistry

Under deep pentobarbital anesthesia (100 μg/g of body weight, i.p.), mice were perfused with 4% paraformaldehyde in 0.1 M phosphate buffer, and processed for parasagittal microslicer sections (50 μm in thickness). After permeabilization and blocking of nonspecific binding of antibodies, the rat antibody

against GFP to visualize virus-infected PCs, the mouse antibody against calbindinD28K to label PCs and the rabbit antibody against VGluT2 (Frontier Institute; 1/200) to label CF terminals were incubated overnight. After incubation with secondary antibodies (anti-rat Alexa Fluor488 antibody; anti-mouse Cy5 antibody, Jackson, 1/300; anti-rabbit Cy3 antibody, Jackson, 1/300), the immunolabeled sections were washed and then examined with a confocal laser scanning microscope (FV10i, Olympus).

Immunocytochemistry

HEK293T cells in a 24-well dish were transfected using X-tremeGENE 9 reagents (Roche) with 250 ng of pCL20c-L7 vectors as indicated in Figures S4 and S5. Three days after the transfection, the cells were fixed. After permeabilization, blocking and application of primary (mouse anti-Arc antibody, Santa Cruz; 1/100) and secondary (donkey anti-mouse Cy3 antibody, Jackson; 1/300) antibodies, the fluorescence signals were examined with a confocal laser scanning microscope (LSM 510, Zeiss).

Real-Time PCR

Total RNA was harvested from P9 and P16 cerebella obtained from 3 mice for each age, using the RNeasy mini kit and RNase-free DNase set (QIAGEN). Reverse transcription was performed using SuperScript III (Invitrogen). Quantitative RT-PCR using SYBR Premix Ex Taq (TAKARA) was performed on an ABI Prism 7900 according to the manufacturer's instructions. The following primer pairs were used for this study: 5'-GGTGAGCTGAAGCCACAAAT-3' (forward) and 5'-TTCACTGGTATGAATCACTGCTG-3' (reverse) for amplification of Arc; 5'-TCCTCCTCAGACCGCTTTT-3' (forward) and 5'-CCTGGTTCATCATCGCTAATC-3' (reverse) for amplification of hypoxanthine guanine phosphoribosyl transferase (HPRT, internal standard); and 5'-CCTTGAGATCAACACGTACCAG-3' (forward) and 5'-CGCCTGTACACTCCACCAC-3' (reverse) for amplification of glyceraldehydes-3-phosphate dehydrogenase (GAPDH, internal standard). Relative expression levels were determined according to the $2^{-\Delta\Delta Ct}$ method (Applied Biosystems).

SUPPLEMENTAL REFERENCES

Amarzguioui, M., Rossi, J.J., and Kim, D. (2005). Approaches for chemically synthesized siRNA and vector-mediated RNAi. FEBS. Lett. *579*, 5974-5981.

Boyden, E.S., Zhang, F., Bamberg, E., Nagel, G., and Deisseroth, K. (2005). Millisecond-timescale, genetically targeted optical control of neural activity. Nat. Neurosci. *8*, 1263-1268.

Hamacher-Brady, A., Brady, N.R., and Gottlieb, R.A. (2006). Enhancing macroautophagy protects against ischemia/reperfusion injury in cardiac myocytes. J. Biol. Chem. *281*, 29776-29787.

Hanawa, H., Kelly, P.F., Nathwani, A.C., Persons, D.A., Vandergriff, J.A., Hargrove, P., Vanin, E.F., and Nienhuis, A.W. (2002). Comparison of various envelope proteins for their ability to pseudotype

lentiviral vectors and transduce primitive hematopoietic cells from human blood. Mol. Ther. *5*, 242-251.

Hashimoto, K., and Kano, M. (2003). Functional differentiation of multiple climbing fiber inputs during synapse elimination in the developing cerebellum. Neuron *38*, 785-796.

Hashimoto, K., Tsujita, M., Miyazaki, T., Kitamura, K., Yamazaki, M., Shin, H.S., Watanabe, M., Sakimura, K., and Kano, M. (2011). Postsynaptic P/Q-type Ca^{2+} channel in Purkinje cell mediates synaptic competition and elimination in developing cerebellum. Proc. Natl. Acad. Sci. USA *108*, 9987-9992.

Hashimoto, K., Yoshida, T., Sakimura, K., Mishina, M., Watanabe, M., and Kano, M. (2009). Influence of parallel fiber-Purkinje cell synapse formation on postnatal development of climbing fiber-Purkinje cell synapses in the cerebellum. Neuroscience *162*, 601-611.

Kawashima, T., Okuno, H., Nonaka, M., Adachi-Morishima, A., Kyo, N., Okamura, M., Takemoto-Kimura, S., Worley, P.F., and Bito, H. (2009). Synaptic activity-responsive element in the Arc/Arg3.1 promoter essential for synapse-to-nucleus signaling in activated neurons. Proc. Natl. Acad. Sci. USA *106*, 316-321.

Konnerth, A., Llano, I., and Armstrong, C.M. (1990). Synaptic currents in cerebellar Purkinje cells. Proc. Natl. Acad. Sci. USA *87*, 2662-2665.

Li, X., Zhao, X., Fang, Y., Jiang, X., Duong, T., Fan, C., Huang, C.C., and Kain, S.R. (1998). Generation of destabilized green fluorescent protein as a transcription reporter. J. Biol. Chem. *273*, 34970-34975.

Miyazaki, T., Hashimoto, K., Shin, H.S., Kano, M., and Watanabe, M. (2004). P/Q-type Ca^{2+} channel α1A regulates synaptic competition on developing cerebellar Purkinje cells. J. Neurosci. *24*, 1734-1743.

Nagai, T., Ibata, K., Park, E.S., Kubota, M., Mikoshiba, K., and Miyawaki, A. (2002). A variant of yellow fluorescent protein with fast and efficient maturation for cell-biological applications. Nat. Biotechnol. *20*, 87-90.

Okuno, H., Akashi, K., Ishii, Y., Yagishita-Kyo, N., Suzuki, K., Nonaka, M., Kawashima, T., Fujii, H., Takemoto-Kimura, S., Abe, M.*, et al.* (2012). Inverse synaptic tagging of inactive synapses via dynamic interaction of Arc/Arg3.1 with CaMKIIβ. Cell *149*, 886-898.

Sawada, Y., Kajiwara, G., Iizuka, A., Takayama, K., Shuvaev, A.N., Koyama, C., and Hirai, H. (2010). High transgene expression by lentiviral vectors causes maldevelopment of Purkinje cells *in vivo*. Cerebellum *9*, 291-302.

Szymczak, A.L., Workman, C.J., Wang, Y., Vignali, K.M., Dilioglou, S., Vanin, E.F., and Vignali, D.A. (2004). Correction of multi-gene deficiency *in vivo* using a single 'self-cleaving' 2A peptide-based retroviral vector. Nat. Biotechnol. *22*, 589-594.

Torashima, T., Okoyama, S., Nishizaki, T., and Hirai, H. (2006). *In vivo* transduction of murine cerebellar Purkinje cells by HIV-derived lentiviral vectors. Brain Res. *1082*, 11-22.

Uesaka, N., Mikuni, T., Hashimoto, K., Hirai, H., Sakimura, K., and Kano, M. (2012). Organotypic coculture preparation for the study of developmental synapse elimination in mammalian brain. J. Neurosci. *32*, 11657-11670.